Microindentation and Nanoindentation Studies of Aging in Pressure-Sensitive Adhesives

Adriana Paiva,† Nina Sheller, and Mark D. Foster*

Maurice Morton Institute of Polymer Science, The University of Akron, Akron, Ohio 44325-3909

Alfred J. Crosby and Kenneth R. Shull

Department of Materials Science and Engineering, Northwestern University, Evanston, Illinois 60208

Received February 8, 2000; Revised Manuscript Received January 10, 2001

ABSTRACT: Microindentation and nanoindentation measurements of model pressure-sensitive adhesives have been used along with scanning probe imaging to follow changes in properties with aging. One blend that is initially miscible stiffens markedly with time for tackifier loadings above a certain value. Lateral phase segregation at the surface is seen for some of the blends along with strong increases in stiffness. Changes with time are less pronounced in the miscible blend with a tackifier stabilized by hydrogenation. While microindentation provides quantitative measurement of changes in overall stiffness and adhesive performance, nanoindentation provides lateral resolution of the changes near the surface. Of the techniques used here, phase detection mode scanning probe imaging provides the most highly surface selective means of noting changes in properties with aging.

Introduction

Pressure-sensitive adhesives (PSAs) are an important class of materials with mechanical and adhesive properties that depend on the microstructure of the films in which these materials are typically used. Adhesives that are denoted as PSAs have the specific properties that they wet a surface quickly under application of light pressure and resist detachment with clean removal.[1] Typically these special properties are obtained by mixing a base resin (a high molecular weight polymer) with small bulky molecules called tackifiers. Bulk phase separation[2−4] and surface segregation[5,6] are among the phenomena that determine adhesive performance by impacting the adhesive film microstructure. Both have already drawn the attention of the scientific community, but their roles in the mechanism of tackification are still not well understood.

In this study we focus on model PSAs created from two model resins, a model tackifier, and a commercial tackifier. Chemical structures for these PSA components are given in Figure 1. Anionically polymerized polyisoprene (PI) is a model for synthetic PI and natural rubber resins. The poly(ethylenepropylene) (PEP) model resin, obtained by hydrogenation of a PI, can be more thermally stable than PI. The *n*-butyl ester of abietic acid (nBEAA) is a model tackifier representative of an entire class of tackifiers derived from wood rosin[7] and similar in properties to lower molecular weight commercial tackifiers. Pentalyn H is a commercial tackifier. It is also derived from wood rosin but contains the wide variety of components characteristic of commercial materials and has been hydrogenated to improve its oxidative stability. The predominant component in the mixture is the Pentaerythritol ester of hydrogenated abietic acid shown in Figure 1. Because of the higher molecular weight of this primary component, the T_g of Pentalyn H is much higher than that of nBEAA.

† Current address: 3M Company, St. Paul, MN.

* Corresponding author: phone (330) 972-5323; Fax (330) 972-5290; e-mail foster@polymer.uakron.edu.

The primary objective of this study was to characterize the effect of aging on the behavior of three model PSAs made from these components. Aging can be accompanied by oxidative degradation, changes in phase behavior, and surface segregation of one component. The effects of these changes in microstructure were investigated using microindentation and nanoindentation, two techniques that probe the adhesive structure and properties on different scales as suggested by Figure 2. Microindentation has the advantage of providing quantitative measurement of the apparent work of adhesion (W_{adh}). Quantitative analysis is possible because in addition to measuring the load and displacement the area of contact is imaged. These measurements provide an overall characterization of the adhesives, since they average over thousands of square micrometers in the lateral direction, and during the indentation the entire thickness of a film is typically perturbed. Nanoindentation with an atomic force microscope, on the other hand, probes behavior on a smaller scale. Those experiments allow one to look at contributions from different phases and collect information on properties and structure that is more heavily weighted with contributions from the near surface region of the film. Spatial resolution is gained at the expense of quantitation since in nanoindentation the contact area is not directly visualized. (In principle, it is possible to estimate these quantities with elastic materials, but for highly viscoelastic materials the currently available approximations are of questionable value.) However, using AFM, the results of the nanoindentation measurements can be supplemented with imaging information that is, in some cases, even more surface specific than the information from nanoindentation.

Experimental Section

Sample Materials and Preparation. Two different rubbery components were used. The polyisoprene (PI) had a weight-average molecular weight of 210 000 g/mol and a polydispersity index of less than 1.1 and was used with 0.1% antioxidant. It was synthesized by anionic polymerization.

10.1021/ma0002343 CCC: $20.00
Published on Web 02/24/2001

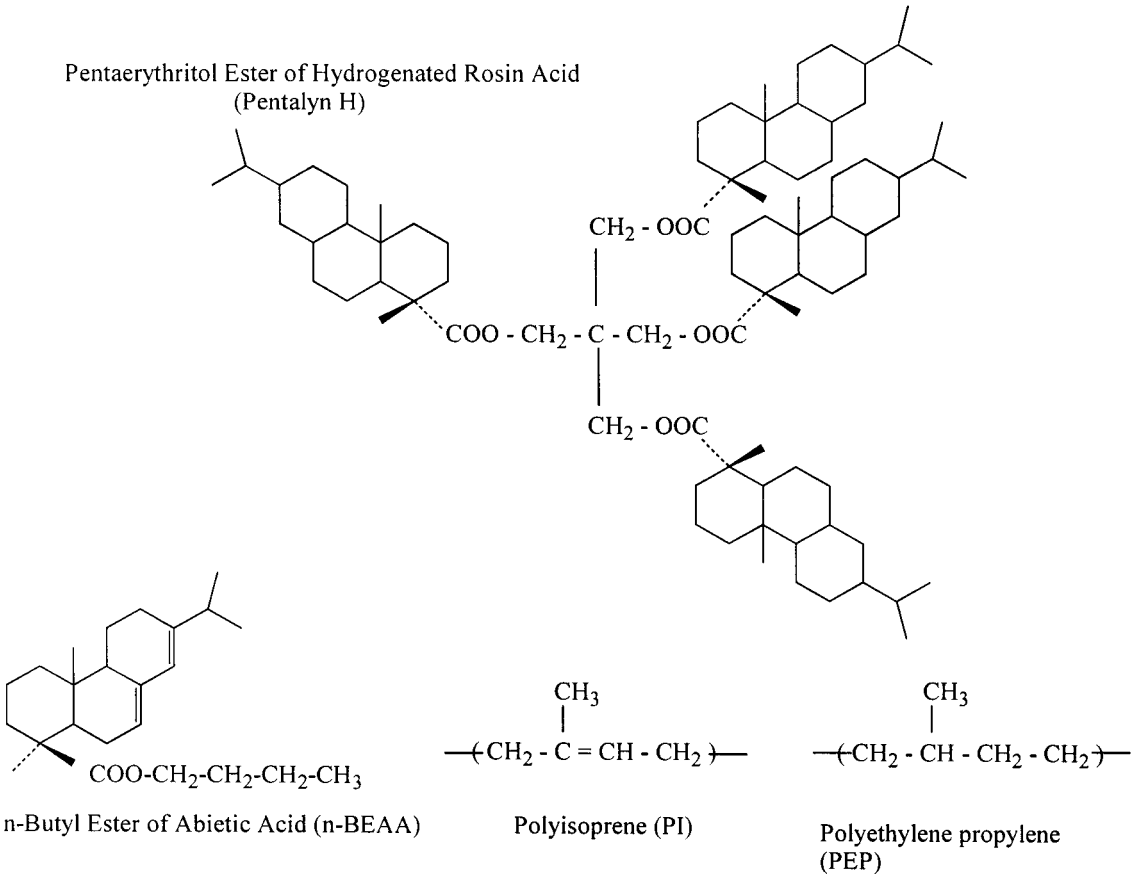

Figure 1. Chemical structures of the tackifiers and rubbery components of the model pressure-sensitive adhesives. PI, PEP, and nBEAA are prepared as pure materials. Pentaerythritol ester is the main component of the Pentalyn H, which is a complex mixture.

Amorphous hydrogenated PI (PEP) with a weight-average molecular weight of 244 000 g/mol and a polydispersity index of 1.7 was obtained from the diimide hydrogenation of PI.[8,9] The *n*-butyl ester of abietic acid (nBEAA) was chosen as a model tackifier because its chemical structure is well-known,[7] it could be readily synthesized, and it belongs to the family of wood rosin derivatives widely used in commercial tackifiers. The commercial tackifier Pentalyn H is a complex mixture but has hydrogenated Pentaerythritol ester of rosin acid as its main component. While the molecular weight and glass transition temperature of nBEAA are 358 g/mol and −45 °C, respectively, those for the commercial tackifier are 1290 g/mol and 54 °C. Thus, two important differences between the two tackifiers are that the molecular weight and glass transition temperature of Pentalyn H are higher. Another difference is that the commercial tackifier is hydrogenated, making it more stable. The hydrogenation also influences the miscibility of the tackifier with the PI.

Adhesion measurements were performed on blends of PEP/nBEAA, PI/nBEAA, and PI/Pentalyn H over a range of composition from 10 to 80 wt % nBEAA. A shorthand notation has been adopted to name the samples. In the case of samples with nBEAA, the sample name contains an abbreviation for the elastomer matrix together with a two-digit number indicating the weight percent loading of nBEAA, e.g., PI/45 and PEP/45. For samples with the Pentalyn H tackifier the number is followed by "H", e.g., PI/45H. Films 50−75 μm in thickness were prepared by solution casting on microscope slides using an Accu Gate fluid spreader. The samples were aged at room temperature and humidity in the dark (e.g., stored in a closed box inside a drawer) and examined 2 weeks and 18 months after being cast using microindentation and after 12 months of aging using nanoindentation.

Previous work in this group[10] has shown freshly cast samples of the PEP/nBEAA system to be phase separated for the compositions considered here. In cast form both the PI/nBEAA and PI/Pentalyn H systems are miscible[11] when freshly cast or aged for only a few weeks or months. The glass transitions of the blends vary somewhat with composition. For example, the T_g of the PI/nBEAA blends measured by DSC (using a temperature ramp rate of 10 °C/min) were −61 °C for pure PI and −53 °C for PI with 45 wt % tackifier.[11] The T_g values of the PI/Pentalyn H blends were slightly higher, with the T_g of PI/45H being −49 °C.

Microindentation. Microindentation experiments were performed as described elsewhere.[12] A glass hemisphere with a diameter of 3 mm was used as the probe. The sample was brought into contact with the glass hemisphere at a displacement rate of 2.5 μm/s for the data acquired when the samples were 2 weeks old and 3.6 μm/s for the data acquired at 18 months of aging. This small discrepancy in the displacement does not significantly affect the results, so that quantitative comparison of results obtained at the different aging times is still possible. When a maximum compressive load of 25 mN was reached, the sample was held in contact with the hemisphere for 1 s, after which unloading started at the same rate of displacement as was used for the loading portion of the test.

Scanning Probe Microscopy (SPM) Measurements (Imaging and Nanoindentation). SPM measurements were performed as described in detail elsewhere.[13] The instrument was an Autoprobe M5 from Park Scientific Instruments. Topographic (AFM) and friction (LFM) images of the samples' surfaces were obtained under ambient conditions in contact mode according to established procedures.[14−16] Measurements were also performed in intermittent contact mode to obtain topographic and phase images. Phase detection microscopy (PDM) can provide enhanced contrast compared to topographic imaging based on variations in composition, adhesion, friction, and viscoelasticity.[16]

Local adhesive and viscoelastic properties were measured by nanoindenting the sample using the tip of the AFM as the

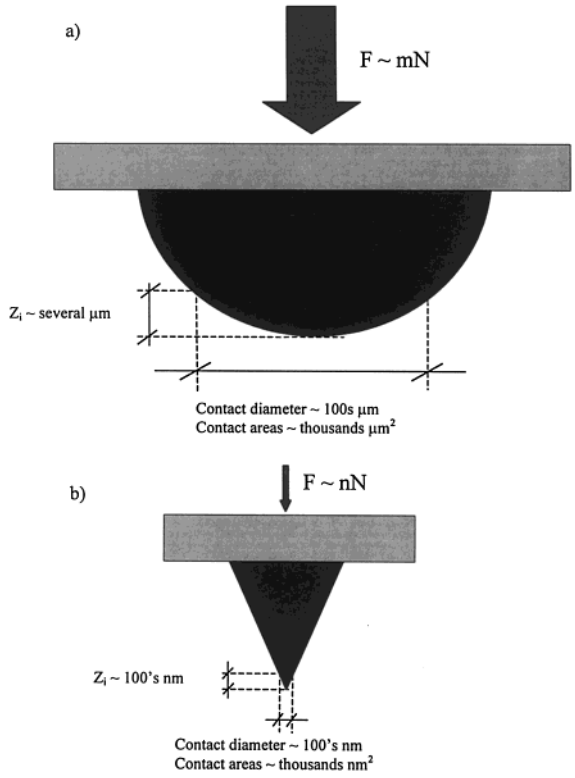

Figure 2. Schematic comparison of the surface adhesion techniques: (a) microindentation; (b) nanoindentation. The penetration depth characteristic of each is noted as Z_i.

probe. Force−distance ($F-\delta$) curves were acquired by applying a displacement rate of 2.5 μm/s to the end of the cantilever opposite the tip. The distance, δ, is the true distance from the nominal film surface after correcting for deflection of the cantilever. A single V-shaped silicon cantilevers (Ultralever, Park Scientific Instruments) with a conical tip having a radius of curvature of 10 nm was used for all experiments. The spring constant of the cantilever, measured experimentally by indentation into a rigid substrate, was determined to be 1.45 N/m. Images and $F-\delta$ curves were obtained after the samples had been aged for 12 months. It was not possible to readily control either the maximum penetration depth or maximum force. Rather, the commercial software allows for a constant overall travel of the piezo, which was set to equal 0.5 μm. Variation in actual penetration depths therefore led to variations in maximum force as well as total energy dissipated in the loading and unloading cycle.

Results

Imaging. Topographic, friction, and phase images were taken with SPM when the samples had been cast for 1 year. SPM images for the PEP/nBEAA samples have been reported in detail in earlier publications.[13,17] We summarize the key results here for ease of comparison. Topographic imaging revealed the character of the phase-separated morphology at the surface and how it changed both with composition and with aging. With the exception of the blend with 60 wt % nBEAA, the blends showed various sorts of morphologies with tackifier-rich domains distributed in polymer-rich matrices. With aging the domain structure was seen to coarsen. The PEP/60 sample displayed a unique behavior. Its surface was uniform even though the bulk of the sample was phase-separated, indicating a surface region of composition distinct from that of the bulk. This uniform surface persisted with aging.

On the basis of optical observations, both the PI/nBEAA and PI/Pentalyn H samples still appeared miscible in the bulk after 12 months. AFM imaging of all the PI/Pentalyn H blends showed the surfaces to be uniform as well. Some lateral segregation at the surface appeared for two of the PI/nBEAA samples, though. The samples with compositions of 10, 30, and 80 wt % tackifier showed uniform surfaces, and these surfaces were still uniform after 17 months. The PI/45 blend had a well-developed two-phase morphology at the surface after 12 months as imaged in Figure 3. Figure 3a presents a topographic image of PI/45 acquired in contact mode. Figure 3b,c presents friction images acquired in opposite scanning directions. Parts d and e of Figure 3 are intermittent contact images of topography and phase, respectively, of a different location on the sample. The topographic image offers hints of the presence of a phase-separated structure, but the morphology is not well resolved. In contrast, the friction and phase images resolve the presence of the lateral variations well. Bright areas in Figure 3b correspond to high-friction regions while dark areas correspond to low-friction regions of the sample. The opposite is true for Figure 3c. The reversal in contrast with scanning direction indicates that there are real differences in friction between the domains and the matrix. One can even observe differences in friction within the domains (i.e., the presence of domains within domains). The regularly shaped circular regions inside the domains had lower friction than did the rest of the domains.

Phase detection microscopy seems to be very sensitive to changes in sample properties and therefore often is characterized by extraordinary contrast, though it is difficult at present to assign this to differences in a specific property. It is thought that changes in phase are related to differences in energy dissipation in the sample.[18] Figure 3e shows the phase image acquired for PI/45 from a different spot on the sample. In the particular case of these samples the domains appearing bright in the image are stiffer than the matrix. PDM images did not show differences in mechanical properties within the domains as the friction images did, but differences in stiffness between the domains and the matrix were revealed. Unfortunately, we do not have images of these PSAs at time zero because at that time the samples of all compositions were so sticky that the tip stuck to the sample and imaging was impossible. However, one can make the qualitative statement that the surfaces of the samples became less adhesive during the first 12 months of aging. Topographic and friction images taken of the PI/45 sample at 17 months showed a very similar morphology with little apparent change in the diameters (ca. 1 μm) of the circular domains.

The surface of the PI/60 sample was not quite uniform at 12 months, showing ill-defined features of irregular, small (diameter < 0.5 μm) domains. There were populations of two types of domains (as in PEP/30[13]): one type with friction lower than that of the matrix and one with friction higher than that of the matrix. When the sample was imaged again at 19 months, approximately circular domains of diameter $\sim$1.5 μm appeared at the surface.

Microindentation. Microindentation measurements provided quantitative information on changes in the films' behavior with composition and time. The area enclosed by the loading and unloading curves is a direct measure of the amount of energy required to remove the probe from the adhesive film. This area can be converted to a figure of merit, the apparent work of adhesion, W_{adh}, by dividing the energy by the maximum

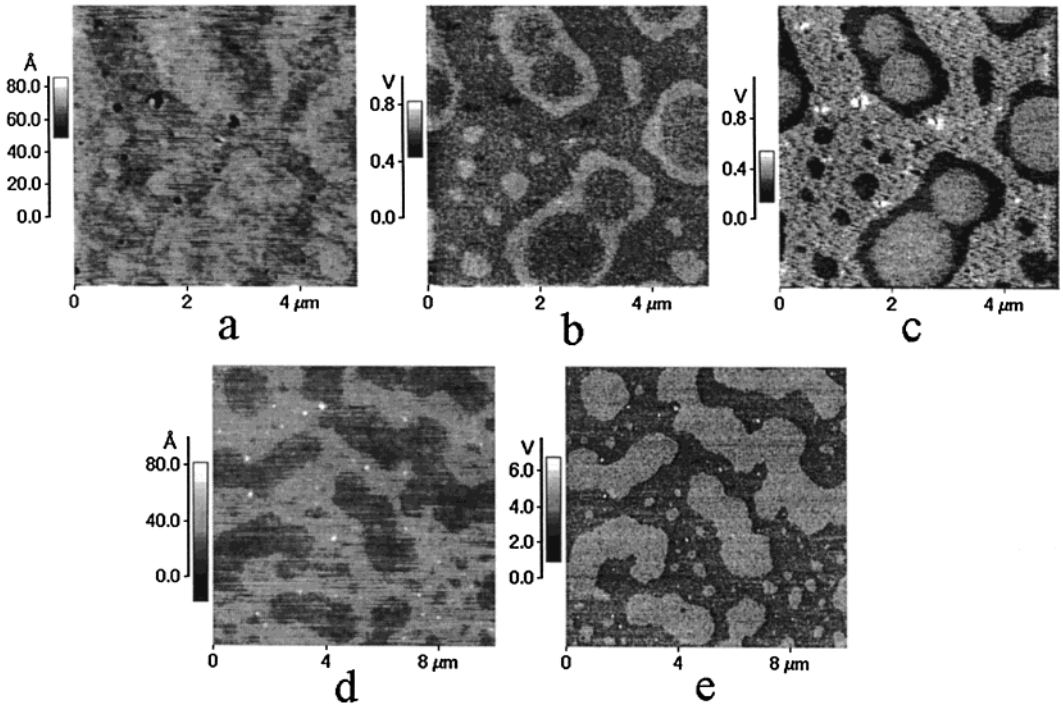

Figure 3. Scanning probe microscopy images of PI/45: (a) topographic image in contact mode; (b, c) LFM images in forward and reverse directions, respectively; (d) topographic image in intermittent contact mode; (e) phase image. Topographic images do not resolve the lateral variations very well. High contrast is observed in the LFM and phase images. Images a−c were all acquired at the same spot on the sample. Images d and e were acquired at another location.

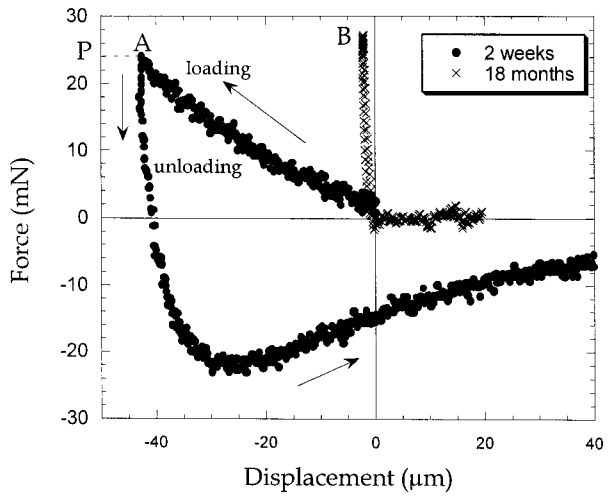

Figure 4. Force−displacement curves measured by microindentation for the PI/45 sample (●) 2 weeks after casting and (×) 18 months after casting. The aged film is much stiffer, and the adhesion energy has dwindled to nearly zero.

contact area established during the loading portion of the test. The work of the adhesion reflects both the influence of the character of the surface and that of dissipative processes in the bulk. The values reported are average values of measurements done in three different areas of each sample. The variation among measurements was about 10%.

Figure 4 shows two representative tack curves, corresponding in this case to the PI/45 sample after 2 weeks and 18 months of aging. The loading curve starts where a measurable force is detected and continues to the point of maximum compression (points A and B in Figure 4 for the sample at 2 weeks and 18 months, respectively). After the maximum force is obtained, the unloading begins. With aging the $F-\delta$ curve shows a sharp increase in stiffness of the film. The changes in stiffness result not only in large differences in penetration (which are clear from the plot) but also in differences in contact area that are not shown but accounted for in the calculation of W_{adh}. After aging one also sees a marked change in the behavior upon retraction. When the indenter is retracted from the fresh sample, the film adheres tenaciously to it. The force goes through a broad minimum and then returns only very gradually to zero as substantial energy is dissipated within the comparatively large volume of adhesive that has been perturbed. This behavior yields a large area between the curves corresponding to a large adhesion energy. In contrast, in the aged sample the penetration is small, and the indenter comes away from the adhesive film with very little resistance. The bulk dissipative mechanism invoked in the fresh sample does not come into play here. The adhesion energy, even after normalization by the maximum contact area, is very small in this case.

The behavior of the curves for all other experiments is summarized by reporting two values, W_{adh}, and an effective modulus, E_p. This effective modulus was derived from the load/displacement curves by utilizing the following expression derived from finite element results:[19]

$$E_p = \left(\frac{9PR}{16a^3}\right)\left(1 + 0.33\left(\frac{a}{h}\right)^3\right)^{-1} \quad (1)$$

where P and a are the force and contact radius at the point of maximum compression, R is the radius of curvature of the indenter (1.5 mm in our case), and h is the thickness of the adhesive film. The values of E_p are clearly only useful for qualitative comparison as the adhesives considered here showed a decidedly viscoelastic behavior, and some samples showed phase separation as well (though the contact areas in microindentation provide averaging over many domains). We

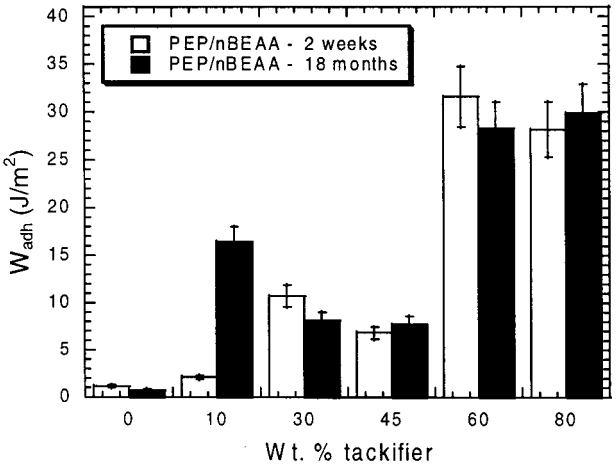

Figure 5. Work of adhesion for different compositions of PEP/nBEAA at 2 weeks and 18 months aging.

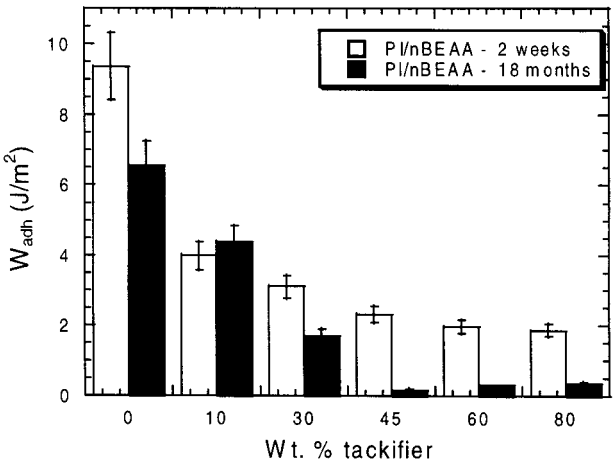

Figure 6. Work of adhesion for different compositions of PI/nBEAA at 2 weeks and 18 months aging. A marked decrease with aging is observed for compositions of 45 wt % tackifier and above.

estimate the uncertainty in E_p could be as large as a factor of 2.

Values of W_{adh} for all the compositions of PEP/nBEAA, PI/nBEAA, and PI/Pentalyn H at 2 weeks and 18 months are summarized in Figures 5, 6, and 7, respectively. The changes in stiffness with aging for the PEP/nBEAA blends are shown in Figure 8 along with the results for the other two systems. The significance of these results is addressed in the Discussion section.

Nanoindentation. Force−displacement curves obtained by nanoindentation for a series of PI/nBEAA and PI/Pentalyn H blends are shown in Figures 9 and 10, respectively. These curves are conceptually similar to the tack curves obtained by microindentation, although a quantitative analysis was not attempted for a variety of reasons. Most importantly, the detailed contact area between the tip and the surface is not known for these experiments. Qualitatively, however, one can argue that the slope of the unloading curve at the beginning of unloading should be related to sample stiffness for samples that are less stiff than the cantilever. This stiffness does vary somewhat with penetration depth, and since penetration depth was not rigorously controlled, only large changes in stiffness are readily discernible in the data here.

Perturbation of the surface by the imaging step, which immediately preceded the nanoindentation step, also

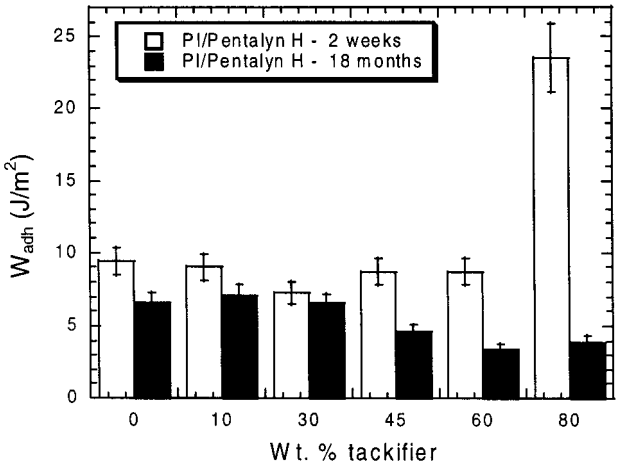

Figure 7. Work of adhesion for different compositions of PI/Pentalyn H at 2 weeks and 18 months aging. The largest decrease is observed for PI/80H.

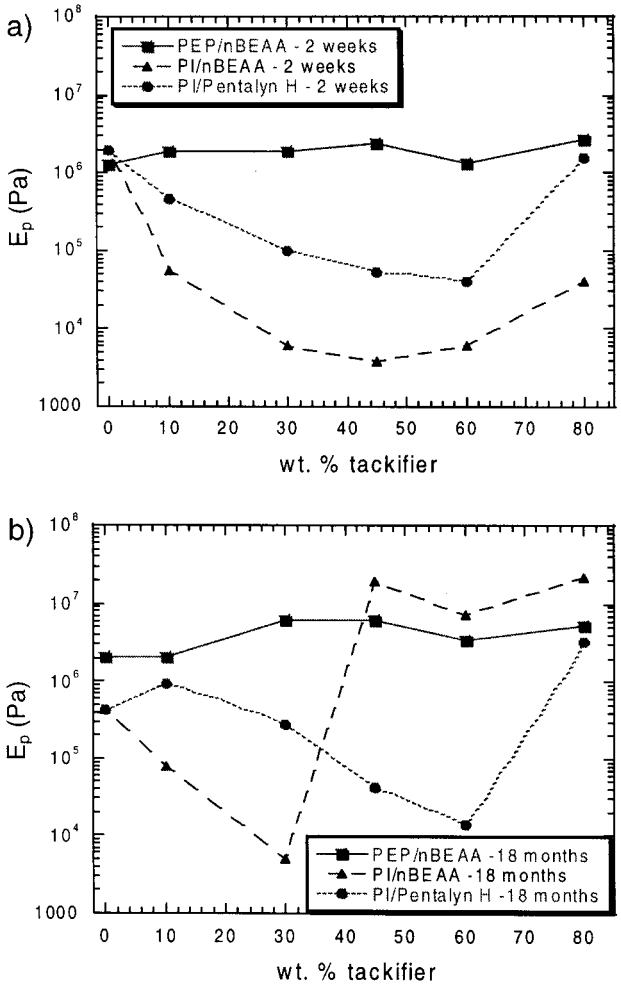

Figure 8. Effective elastic modulus for different compositions of tackifier at (a) 2 weeks and (b) 18 months.

affects the results. When the tip was retracted from the surface at the end of imaging step, the adhesive often clung tenaciously to the tip. The stress exerted by this material relaxed over time but was sometimes still present at the beginning of the nanoindentation experiment. This effect was responsible for the negative (tensile) forces observed for some samples at large displacements, where the tip was originally approaching the sample. By the time the zero displacement point was

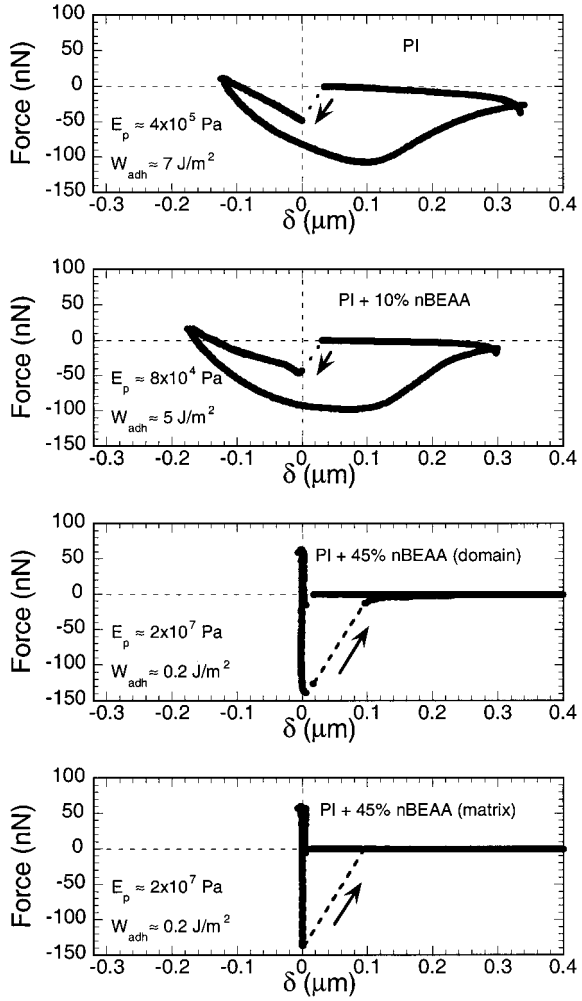

Figure 9. Force−displacement curves measured with the tip of an AFM for PI/nBEAA blends at different compositions. The composition with 45% tackifier has a two-phase morphology at the surface. Values of E_p and W_{adh} determined from microindentation are shown in the lower left corner for reference.

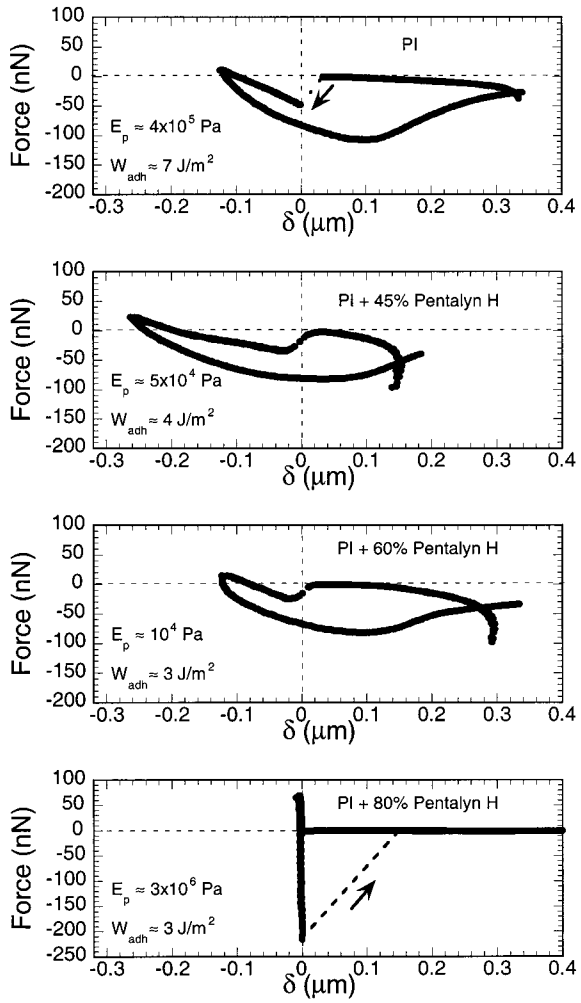

Figure 10. Force−displacement curves measured with the tip of an AFM for PI/Pentalyn H blends at different compositions. Values of E_p and W_{adh} determined from microindentation are shown in the lower left corner for reference. Note the larger scale on the ordinate for all plots as compared to Figure 9. In particular, the scale for the sample with 80 wt % Pentalyn H is larger.

reached in the loading curves, the fibril remaining from the imaging had generally relaxed completely. Subsequent $F-\delta$ measurements[20] made on select samples under slightly different conditions to eliminate this artifact showed that its presence did not affect the important features of the $F-\delta$ curves discussed below.

Discussion

As mentioned above, the topographic information indicates that the PEP/nBEAA system is immiscible, whereas the PI/Pentalyn H system shows no signs of phase separation, either in the bulk or at the surface. The PI/nBEAA system shows an intermediate behavior, with phase separation indicated only by surface sensitive probes after long aging times. On the basis of these results, we refer to these three systems as "miscible", "immiscible", or "partially miscible" in the following discussion, which also is organized around this distinction.

Immiscible System: PEP/nBEAA. As shown in Figure 5, W_{adh} varies markedly with composition for the PEP/nBEAA blends, but the changes with aging are generally small. The apparent increase with aging for 10 wt % tackifier is an artifact of limitations in the control of the maximum force obtained during loading. In general, the variation in maximum load from experiment to experiment was about 5 mN, but for the case of the 18 month aged sample at 10 wt % nBEAA the maximum load was particularly high, i.e., 35 mN. The indenter pressed somewhat deeper into the sample, and more bulk dissipation resulted upon unloading.

The moduli for the PEP blends, shown in Figure 8a,b, are of the same order of magnitude for the different compositions. Except for the case of the 10% sample (artifact noted above), the moduli increase slight with aging. We conjecture that the modulus increase is due at least in part to a stiffening of the PEP itself. This was caused by cross-linking among the PEP chains that occurred because a small fraction of cross-linkable moieties were unintentionally incorporated into the chains during diimide hydrogenation.[8] Size exclusion chromatography of the PEP after aging revealed a small increase in polydispersity and mean molecular weight.

Partially Miscible System: PI/nBEAA. Stronger aging effects were seen for the two adhesives made with PI. For the PI/nBEAA system W_{adh} generally decreased with aging, except for the sample with 10 wt % for which there was no change, as shown in Figure 6. Among the three samples with lowest tackifier loading W_{adh} de-

creases with increasing tackifier concentration at both 2 weeks and 18 months. For concentrations of 45, 60, and 80 wt % nBEAA they are the same within the scatter. The decrease in W_{adh} with increasing loading at low concentration looks peculiar for a PSA, but conventional macroscopic (Polyken) probe tack measurements[11] done at 12 months aging (10 mm/s, 1 s contact) showed a respectable maximum tack force (1.4 ± 0.4 kg) at 45 wt % tackifier. The probe tack dropped to nearly zero for the two higher compositions. These macroscopic tack tests probed the behavior of the adhesive at a very different frequency and therefore cannot be compared directly to the microindentation and nanoindentation results but do serve to benchmark the conventional "tackiness" of the blends.

Inspection of the values of E_p shown in Figure 8 reinforces the impression that there is a qualitative difference in composition dependence for "low" tackifier loadings and "high" tackifier loading. At 2 weeks, the modulus decreases sharply as tackifier concentration is increased from 0 to 30 wt %. The nBEAA plasticizes the films. The modulus is similar at 30, 45, and 60 wt % tackifier and increases for 80 wt % nBEAA. The variation in modulus with composition changes remarkedly after an aging time of 18 months. The moduli for loadings of 45, 60, and 80 wt % increase by roughly 3 orders of magnitude. These observations suggest that the reason for lost adhesive energy with aging at the higher compositions is stiffening of the adhesive. Deformation of the adhesive to large strains is not possible, and the bulk energy dissipation responsible for the effective performance of a pressure-sensitive adhesive is minimized.

Nanoindentation measurements were done to further clarify the character of the adhesive stiffening with time. It was anticipated that since nanoindentation probes the film properties in a much smaller volume near the surface, similarities or differences between results from the two techniques would yield hints as to the role of the surface. Also, AFM imaging would allow variations in behavior in the direction parallel to the surface to be detected.

Nanoindentation measurements were done after an aging time of 1 year, because immediately after casting the samples were so sticky that attempts to obtain images were unsuccessful. The key effect evident in the $F-\delta$ curves in Figure 9 is that there is a large increase in contact stiffness in going from the blends with low tackifier loading to the blend at a loading of 45% nBEAA. In fact, the sample with 30% loading was so soft that it could not be imaged without damage, and on the basis of this observation, we argue that the stiffness first decreases somewhat with tackifier loading and then increases. The stiffness observed for the composition of 45 wt % nBEAA and above is considerably larger than that at 30 wt % nBEAA and below. It is not possible to state whether the compositions of 45, 60, and 80 wt % gave distinct behavior because for all these compositions the stiffness of the films exceeds that of the cantilever. What is clear is that the samples with high stiffness as measured by nanoindentation also have low adhesion energies. The penetration of the tip into the films is negligible even though the measurement is being done about 65 °C above the glass transition temperature of the blend. The tackifier-rich domains in the PEP blends[13] likewise had stiffnesses exceeding that of the cantilever. The stiffening is not due to changes in the PI, as the PI itself becomes softer with time due to chain scission.

Nanoindentation measurements were performed in both the matrix and domain regions for the sample with 45% nBEAA. The nanoindentation curves are nearly identical because the cantilever stiffness is lower than that of the film in both regions. This behavior is distinct from that in the PEP blends[17] where the stiffness of the matrix remained slightly smaller than that of the cantilever even after 10 months aging.

Miscible System: PI/Pentalyn H. The effect of aging was different for the PI/Pentalyn H samples, but again the composition of 45 wt % tackifier appeared to separate two regimes of behavior. For the samples aged for 2 weeks W_{adh} is higher for all of the PI/Pentalyn H blends than for the corresponding PI/nBEAA blends. W_{adh} is nearly constant with tackifier loading until the composition of 80 wt % is reached, and then it increases sharply. (In contrast, macroscopic probe tack measurements at 12 months[11] showed a maximum of 1.8 ± 0.4 kg force at 60 wt % with a dramatic drop in tack for 80 wt %.) After aging for 18 months, W_{adh} is still higher for the blends with Pentalyn H. For the pure PI there is a modest loss in W_{adh} with aging to 18 months, while for compositions of 45 wt % and above the losses are larger. The change for the sample with 80 wt % tackifier is quite striking. The more modest changes at the other concentrations are consistent with expectations that the more stable hydrogenated tackifier should reduce changes in adhesion with time. The fact that the value of W_{adh} at 80 wt % changes strongly suggests, on the other hand, that accounting for changes in the tackifier itself with time probably does not fully explain the aging behavior. When studying the moduli estimated for the PI/Pentalyn H blends, one sees that both before and after aging the adhesive is significantly stiffer at 80 wt % than at 60 wt % tackifier (see Figure 8). The 80 wt % blend is slightly stiffer after aging, but the reason that W_{adh} drops so strongly is that the probe completes its detachment from the surface over a much shorter retraction distance, eliminating the large energy dissipation associated with large-scale deformation of the adhesive.

Nanoindentation curves for the PI/Pentalyn H blends are shown in Figure 10. As with microindentation the qualitative character of the $F-\delta$ curve at 80 wt % tackifier is distinct from those at smaller loadings. In contrast to the microindentation results, the stiffnesses appear to increase somewhat for increasing tackifier loading from 45 to 60 to 80 wt %. The sample with 80 wt % tackifier is definitely stiffer than is the cantilever. The initial slope of the unloading curve for the sample with 60 wt % Pentalyn H suggests that it has a stiffness close to that of the cantilever, but it lies enough below that critical value that the sample is still penetrated by the tip. No obvious relationship between the shapes of the curves and the values of W_{adh} from microindentation appears. Even when the surface appears "stiff" the value of W_{adh} is within a factor of 2 of the value for PI.

The fact that a stiffening is seen at the highest tackifier loading in both types of PI blends, despite the fact that the Pentalyn H should be more oxidatively stable, suggests that chemical change in the tackifier alone cannot explain the stiffening. On the other hand, the stiffening is not due to migration alone due to the time scale over which changes are seen. The diffusion of the tackifier has been shown to be sufficiently rapid[10]

so that surface segregation of tackifier could easily occur on a time scale of hours if it were thermodynamically favored. It is also true that phase separation in the bulk or at the surface should be evident at times much shorter than 2 weeks if it is thermodynamically favored in the new samples. We conjecture that the long time aging behavior is due to slow surface enrichment and phase segregation resulting from slow chemical changes in the tackifier and polymer. As the tackifier ages, the blends become less miscible. This would lead first to greater enrichment of one component at the surface and then, at some compositions, to phase separation. The lateral separation in the neighborhood of the surface could precede bulk phase separation.[21] It does not appear that lateral surface segregation is responsible for the stiffening of the surface. The PI/80 sample stiffens markedly even though no lateral surface segregation was observed.

Summary

Measurements of the adhesion properties of model pressure-sensitive adhesives using indentation force−distance measurements and different scanning probe imaging modes reveal not only differences among the three different systems but also changes with time. Microindentation measurements average over larger areas but provide quantitative comparison of the adhesion energy per area. Nanoindentation measurements probe less deeply, effectively weighing the properties close to the surface more heavily. AFM phase detection mode imaging provides the most highly surface selective approach for noting variations in the adhesive mechanical properties but is least readily quantified.

Changes in adhesive stiffness with composition were more pronounced in the miscible systems than in the immiscible system. While there were slight increases in stiffness in some compositions of the immiscible model adhesives with time at the frequency tested, the behavior of both PI-based adhesives changed more substantially. Most notable was a large increase in stiffness over 18 months for the PI/nBEAA blends for nBEAA loadings above 30 wt %. This stiffening degrades the adhesiveness of the films. Both excessive softening and the stiffening can lead to loss of adhesive performance, apparently through the loss of the ability to deform the adhesive to large strains. In the case of the PI/nBEAA blends the stiffening was accompanied by phase segregation at the film surface for only two of three compositions which had large increases in stiffness, suggesting that the lateral phase segregation itself was not the cause of the reduced performance.

Acknowledgment. The authors thank Professor R. P. Quirk, Dr. S. Corona-Galvan, and Dr. R. S. Porzio for providing the polyisoprene and Seung-ho Moon for assistance with preparation of the figures. Research support from the Army Research Office, Contracts DAAH04-95-1-0562 and DAAG55-97-1-0079 (DURIP), is gratefully acknowledged (Akron), as is support from the National Science Foundation through Grant DMR-9975468 (Northwestern).

References and Notes

(1) Pocius, A. V. *Adhesion and Adhesives Technology: An Introduction*, 1st ed.; Hanser-Gardner: Cincinnati, 1997.
(2) Wetzel, F. H. *Rubber Age* **1957**, *82*, 291.
(3) Fujita, M.; Kajiyama, M.; Takemura, A.; Ono, H.; Mizumachi, H. *J. Appl. Polym. Sci.* **1998**, *70*, 771.
(4) Fujita, M.; Kajiyama, M.; Takemura, A.; Ono, H.; Mizumachi, H. *J. Appl. Polym. Sci.* **1998**, *70*, 777.
(5) Bates, R. *J. Appl. Polym. Sci.* **1976**, *20*, 2941.
(6) Andrews, E. H.; Khan, T. A.; Drew, P.; Rance, R. *J. Appl. Polym. Sci.* **1990**, *41*, 595.
(7) Aubrey, D. W. *Rubber Chem. Technol.* **1988**, *61*, 488.
(8) Harwood, H. J.; Russell, D. B.; Verthe, J. J. A.; Zymonas, J. *Makromol. Chem.* **1973**, *163*, 1.
(9) Hahn, S. F. *J. Polym. Sci.* **1992**, *30*, 397.
(10) Paiva, A.; Foster, M. D.; von Meerwall, E. *J. Polym Sci., Part B: Polym. Phys.* **1998**, *36*, 373.
(11) Paiva, A. Ph.D. Thesis, The University of Akron, 1999.
(12) Ahn, D.; Shull, K. R. *Macromolecules* **1996**, *29*, 4381.
(13) Paiva, A.; Sheller, N.; Foster, M. D.; Crosby, A. J.; Shull, K. R. *Macromolecules* **2000**, *33*, 1878.
(14) Sarid, D. *Scanning Force Microscopy with Applications to Electric, Magnetic and Atomic Forces*, 2nd ed.; Oxford University: New York, 1994.
(15) Wiesendanger, R. *Scanning Probe Microscopy and Spectroscopy: Methods and Applications*, 1st ed.; Cambridge University: New York, 1994.
(16) Magonov, S.; Whangbo, M.-H. *Surface Analysis with STM and AFM: Experimental and Theoretical Aspects of Image Analysis*, 1st. ed.; VCH: New York, 1996.
(17) Paiva, A.; Foster, M. D. *J. Adhes.* **2001**, *75*, 145.
(18) Magonov, S. N.; Elings, V.; Whangbo, M.-H. *Surf. Sci. Lett.* **1997**, *375*, L385.
(19) Shull, K. R.; Ahn, D.; Chen, W.-L.; Flanigan, C. M.; Crosby, A. *Macromol. Chem. Phys.* **1998**, *199*, 489.
(20) Jia, S.; Foster, M. D. Unpublished results.
(21) Binder, K. *Acta Polym.* **1995**, *46*, 204.

MA0002343